5-FLUOROURACIL MATRIX TABLETS

6.3.1 Preformulation studies

The following preformulation studies were performed for 5-fluorouracil (5-FU).

a. Solubility

Solubility of 5-fluorouracil (5-FU) was found to be 11.87 gm/L in simulated vaginal fluid pH 4.2 and 12.4 gm/L in phosphate buffer pH 6.8, whereas the solubility of 5-fluorouracil in phosphate buffer pH 7.4 was found to be 12.21 gm/L.

b. Partition coefficient studies

Apparent partition coefficient of 5-fluorouracil determined by octanol/ phosphate buffer pH 6.8 was found to be 0.4 and in simulated vaginal fluid pH 4.2 was found to be 0.6 and in phosphate buffer pH 7.4 was 0.5.

c. Screening studies

The characterization of drugs and polymers were carried out using DSC and FT-IR

Differential Scanning Calorimetry (DSC): DSC studies were carried out for 5-fluorouracil (5-FU) and its combination with polymers in the ratio of 1:1 and the thermograms obtained are presented in Figure 64 and 65. From the thermograms, it is evident that decomposition temperature of 5-fluorouracil (282 °C) when mixed with excipients (282.37 °C). Hence, it can be inferred that there was no interaction between 5-fluorouracil and polymers used in the preparation of tablets.

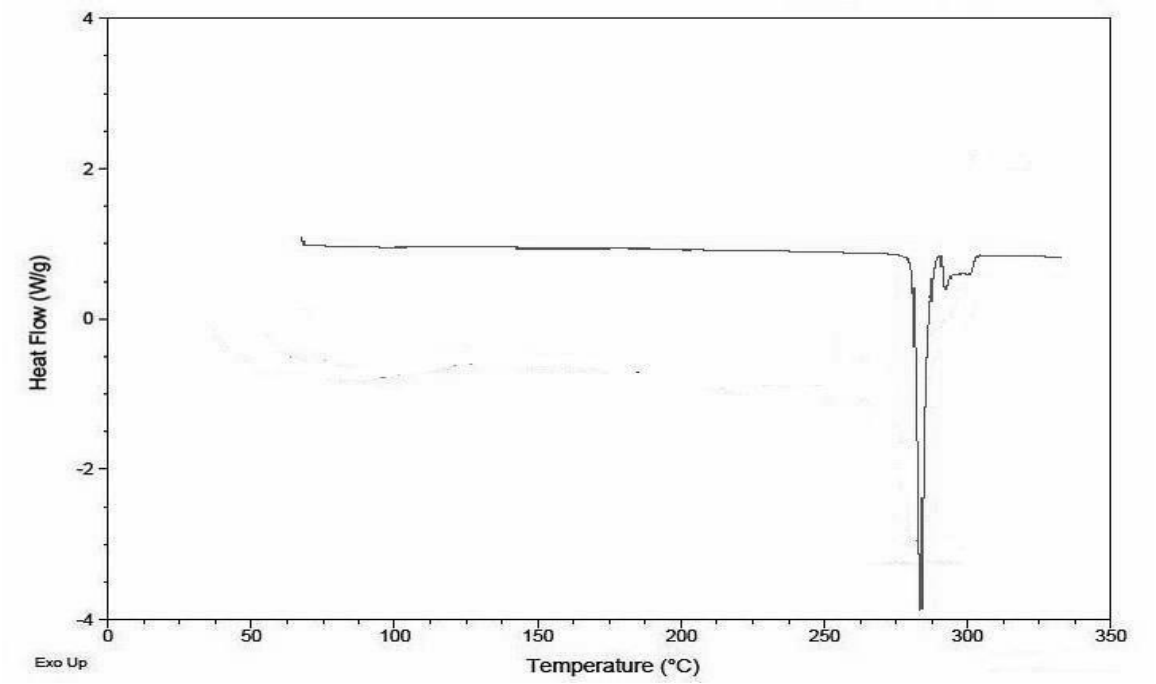

Figure 64: DSC thermogram of 5-fluorouracil (5-FU)

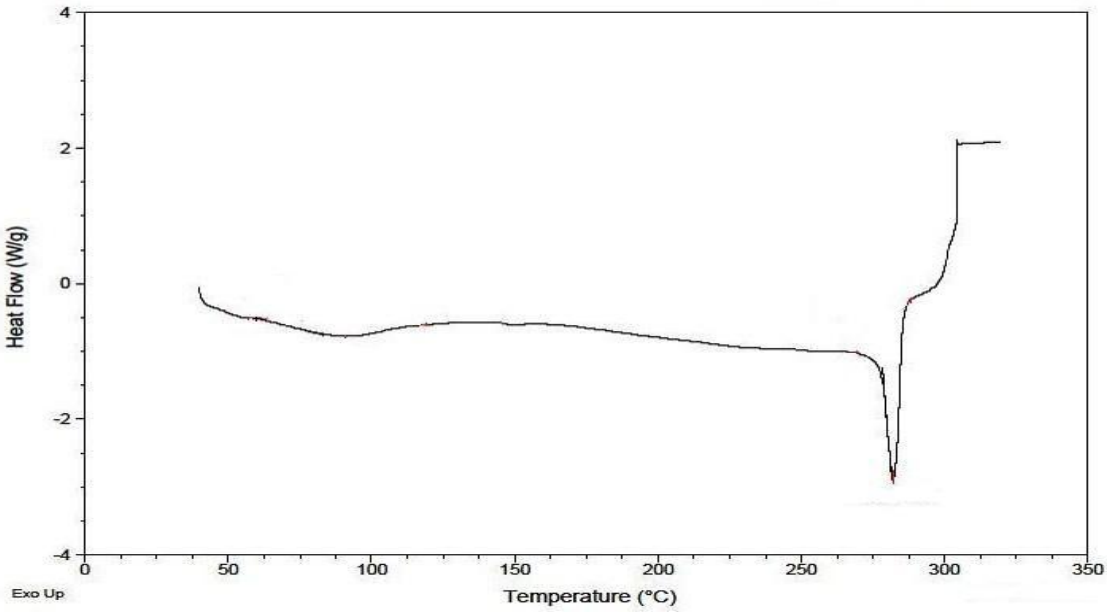

Figure 65: DSC thermogram of 5-fluorouracil (5-FU) with excipients

Fourier transform infrared spectroscopy: The compatibility between the drug and polymer was compared by FT-IR spectra. The position of peak in FT-IR spectra of pure 5-fluorouracil was compared with those in FT-IR spectra of 5-fluorouracil with excipients. It was observed that, there was no disappearance or shift in band position of functional groups in spectrum of 5-fluorouracil alone and with excipients, which proved that 5-fluorouracil and excipients were compatible. Hence, it can be concluded that drug can be used with the selected polymer without causing instability in the formulation. The spectra are reported in Figures 66 and 67. The data is summarized in table 29.

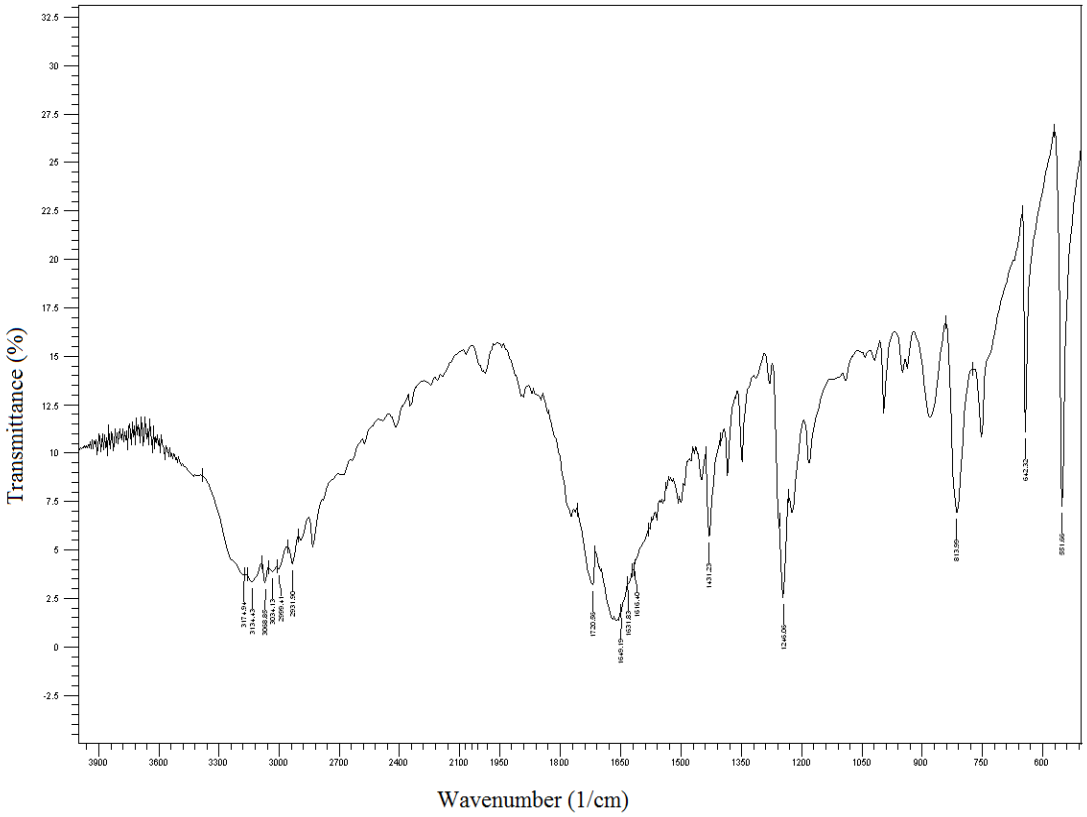

Figure 66: FT-IR Spectra of pure 5-fluorouracil (5-FU)

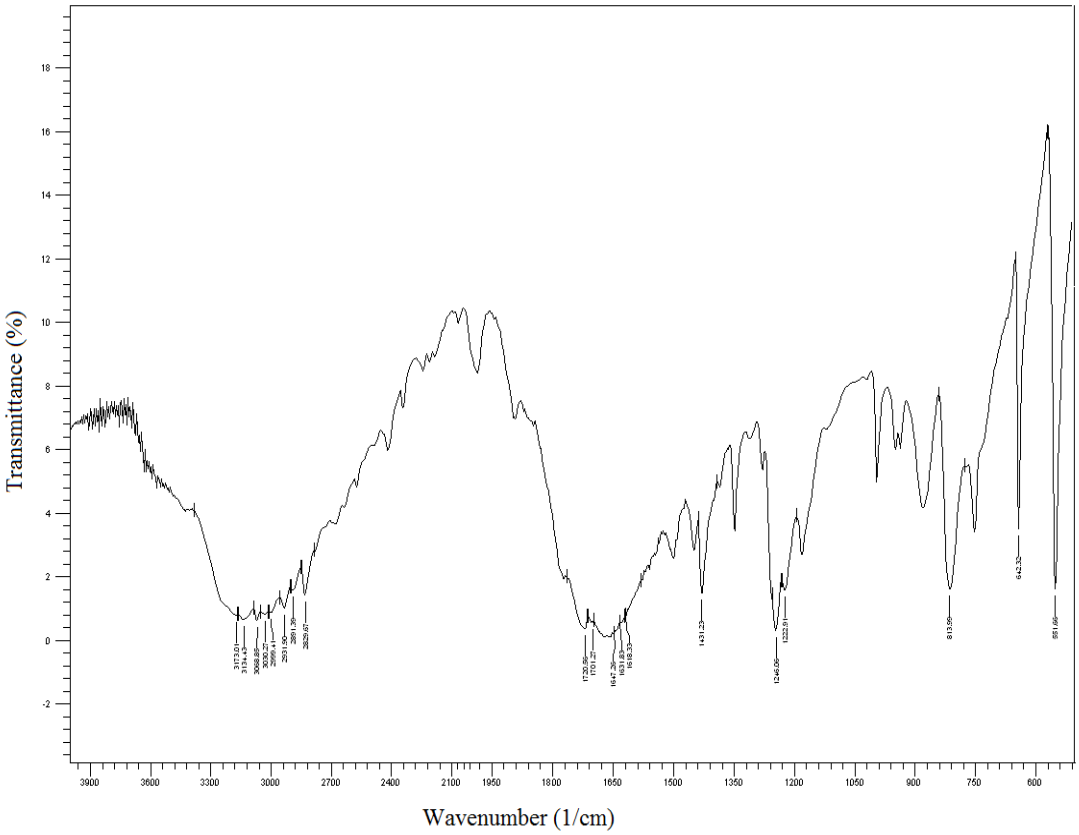

Figure 67: FT- IR Spectra of 5-fluorouracil (5-FU) with excipients

Table 29: FT-IR spectra data of 5-fluorouracil (5-FU) and the formulation

Group	Wavenumber (cm^{-1})	
	Drug	**Formulation**
N-H(Stretching) Free	3173.01	3172.94
C=O(Stretch)	1720.58	1728.32
C-N(stretch)	1649.19	1647.21
C-H (in plane)	1243.03	1239.85
C-O	1180.11	1178.23

6.3.2 Transmittance measurement of chitosan-polycarbopohil (Noveon AA-1) IPEC ratios

The change in transmittance as a function of the ratio of chitosan to polycarbophil was measured to determine the composition of the IPEC, as shown in figure 68.The chitosan aqueous acetic acid solution and the polycarbophil aqueous solution were transparent regardless of their concentration prior to mixing. The supernatant liquid after IPEC formation with various ratios of polymers was taken for transmittance. From ratio 3:1 to 3:3 there was increase in transmittance and from 3:4 to 2:1 ratio there was decrease in transmittance. At 3:3 ratio all the chitosan had reacted with polycarbophil hence there is saturation of electrostatic interaction sites of polycarbophil. Further increase or decrease in concentration of polymers did not exhibit greater interaction. Hence there is decrease in transmittance.

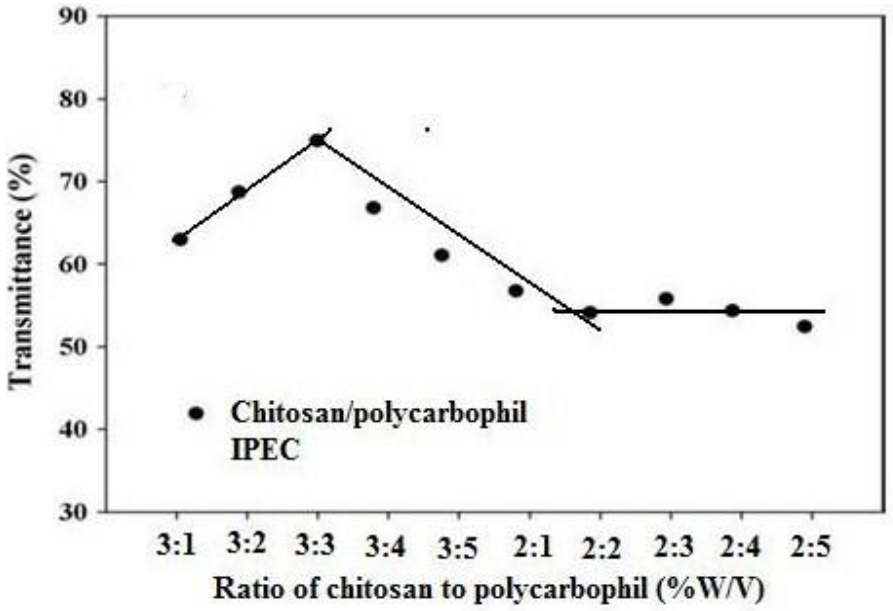

Figure 68: Transmittance of the supernatant solutions of different ratios of chitosan and polycarbophil

6.3.3 Characterization of the chitosan-polycarbophil IPEC

6.3.3.1 Fourier transform infrared spectroscopy (FT-IR)

The FT-IR spectrum of chitosan shows absorption band due to the carbonyl group stretching of the secondary amide appears at 1656 cm^{-1} indicating that chitosan is not totally deacetylated [202]. The bands at 1575, 1421 and 1321cm^{-1} correspond to the N-H bending vibration (amine I), N-H stretching of the amide and ether bonds and the amide III band, respectively [203]. The peaks at 1160, 1075, 1040 cm^{-1} correspond to the bridge oxygen (C-O-C) stretching bands [204]. The FT-IR spectra of chitosan in 2000-1000 cm^{-1} and 1800-1400 cm^{-1} were given in figure 27 and 28 respectively.

In FT-IR spectrum of polycarbophil a strong band at 1715 cm^{-1} assigned to the O–H stretching (hydrogen-bonded). The weak band at 1412 cm^{-1} is due to the symmetric stretching of carboxylate anion (COO^{-}), bands 1228 and 1165cm^{-1} are attributed to the C-O stretching [205]. The FTIR spectra of polycarbophil in 2000-1000 cm^{-1} and 1800-1400 cm^{-1} were given in figure 69 and 70 respectively.

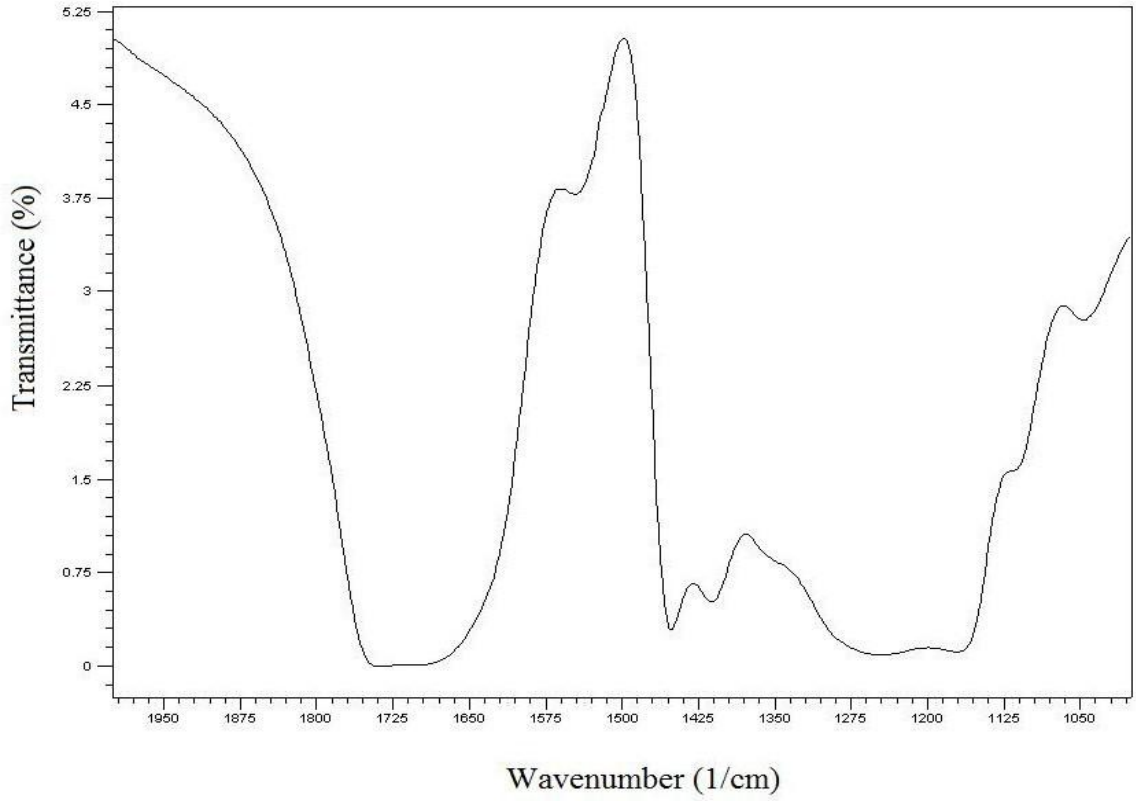

Figure 69: FT-IR spectra of polycarbophil in 2000-1000 cm^{-1}

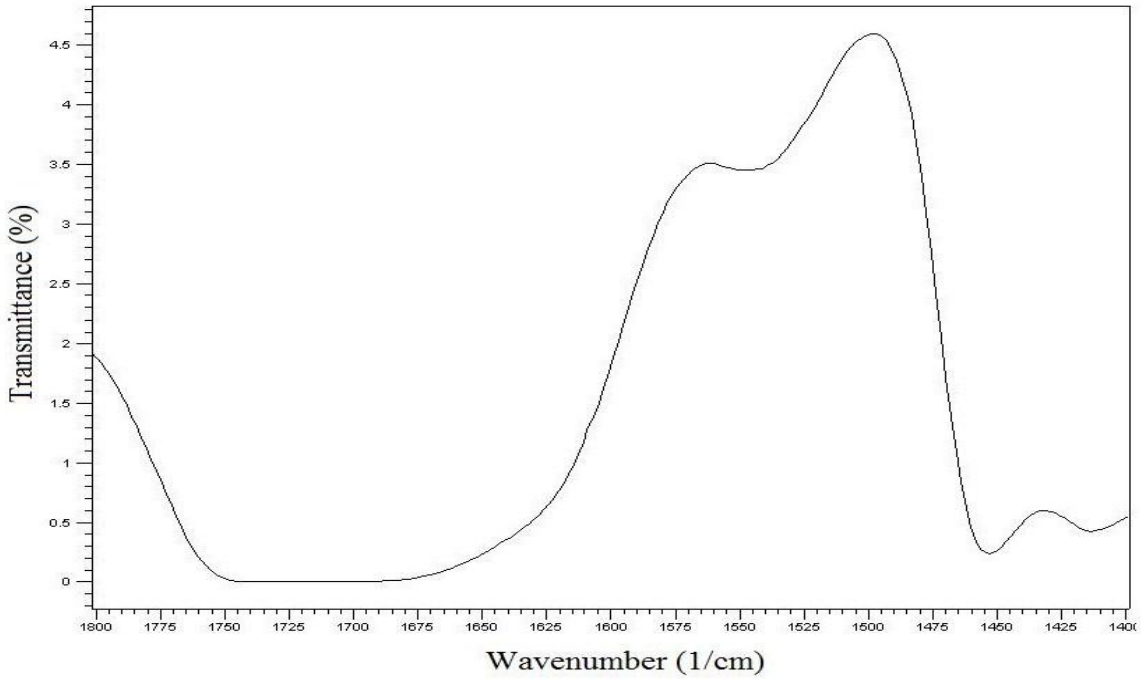

Figure 70: FT-IR spectra of polycarbophil in 1800-1400 cm^{-1}

When two immiscible polymers are brought together, it is expected that the resulting infrared spectrum will be the sum of the spectra of the individual compounds because the polymers will have the same environment. When the polymers are miscible, intermolecular interactions may occur and will be reflected in changes on the infrared spectra of the mixture such as wavenumber shifts, band broadening and new absorption bands that are evidence of the polymers miscibility [206]. For this reason, it is expected to find a characteristic absorption bands of the NH_3^+ and COO^- groups in the FT-IR spectra of IPEC. In IR spectra of Chitosan-polycarbophil IPEC, a new and strong band is observed at 1561 cm^{-1}. This new band can be due to the overlapping of asymmetric COO^- stretching vibration of polycarbophil and the NH_3^+ asymmetric bending vibration of chitosan which is in agreement with literature and located between 1550–1610 cm^{-1} [207]. In addition, another band at approximately 1402 cm^{-1} is a further evidence of the interaction because it is attributed to the symmetric COO^- stretching vibration [208]. The FT-IR spectra of IPEC in 2000-1000 cm^{-1} and 1800-1400 cm^{-1} are given in figure 71 and 72 respectively.

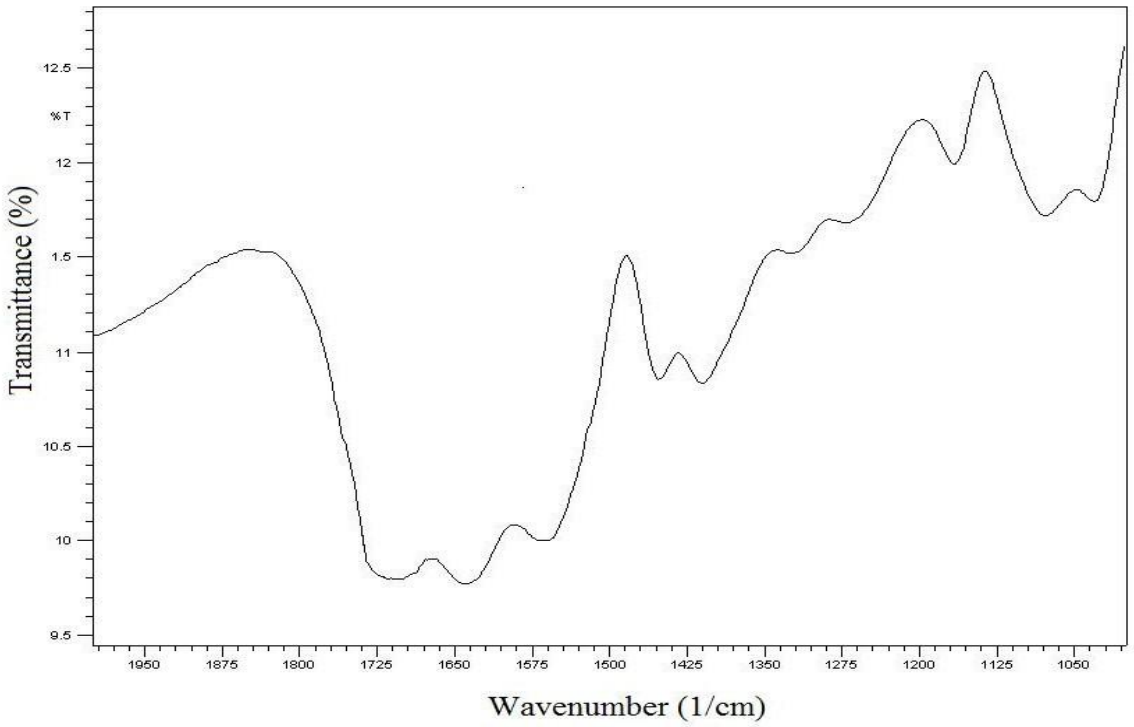

Figure 71: FT-IR spectra of chitosan-polycarbophil IPEC in 2000-1000 cm^{-1}

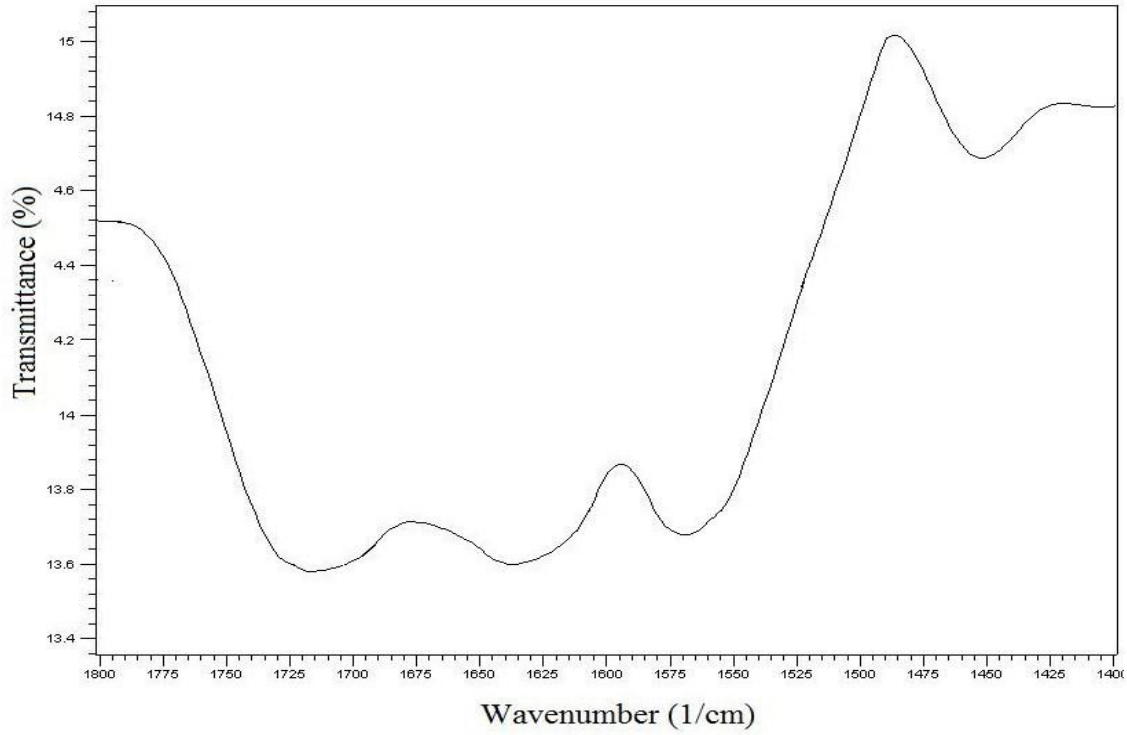

Figure 72: FT-IR spectra of chitosan-polycarbophil IPEC in 1800-1400 cm^{-1}

6.3.3.2 Differential scanning calorimetry (DSC)

Pure chitosan exhibits a endothermic peak at 110 °C associated to the evaporation of absorbed water, a glass transition at 243 °C and an exothermic peak at about 320 °C ascribed to the polymer degradation, including saccharide rings dehydration, depolymerization and decomposition of deacetylated and acetylated chitosan units [209-211]. The DSC thermogram of chitosan is shown in figure 33.

Polycarbophil thermogram exhibits two endothermic peaks at 91 °C and ~245 °C. The first endothermic peak is short and narrow peak assigned to the evaporation of water from hydrophilic groups in the polymers and the second one corresponds to a thermal degradation through intermolecular anhydride formation and water elimination [212,213]. DSC thermogram of polycarbophil is given is figure 73.

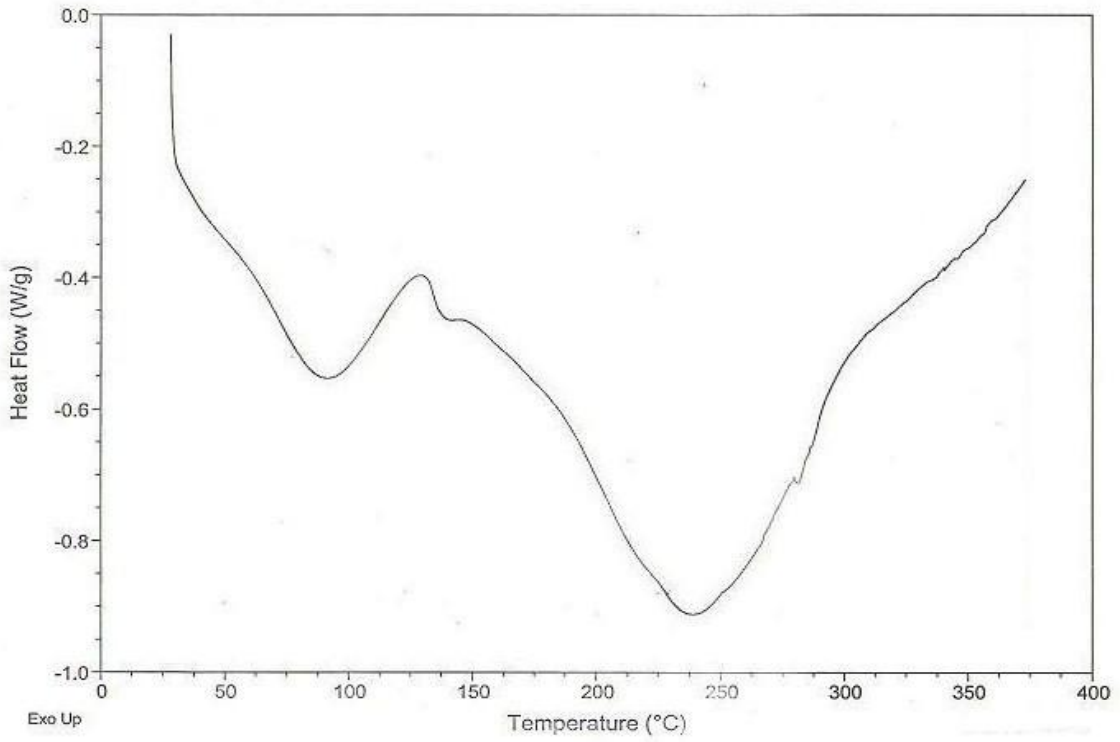

Figure 73: DSC thermogram of polycarbophil

DSC thermogram of IPEC is given in figure 74. The chitosan-polycarbophil IPEC thermogram exhibit four endothermic peaks. The first and second one is associated with the vaporization of water at ~53 °C and ~100 °C in the chitosan polycarbophil IPEC. The third endothermic peak is probably related with the cleavage of the electrostatic interactions between the oppositely charged polymers. A new small broad endotherm at ~270 °C is observed [214]. Although the thermogram of IPEC between chitosan and polycarbophil resembles some aspects of each of the individual starting polymers, the appearance of a new endotherm at ~270 °C is indicative of a compound of distinct thermal behavior properties. Because it is widely accepted that oppositely charged hydrophilic polymers form cross-links between the polymer chains in aqueous solutions, the considerable change in the thermogram is probably an indication of the formation of a complex between chitosan and polycarbophil. The similarities in the thermogram of IPEC and the starting polymers may be explained by some parts of the individual polymer chains in the IPEC that are not cross-linked.

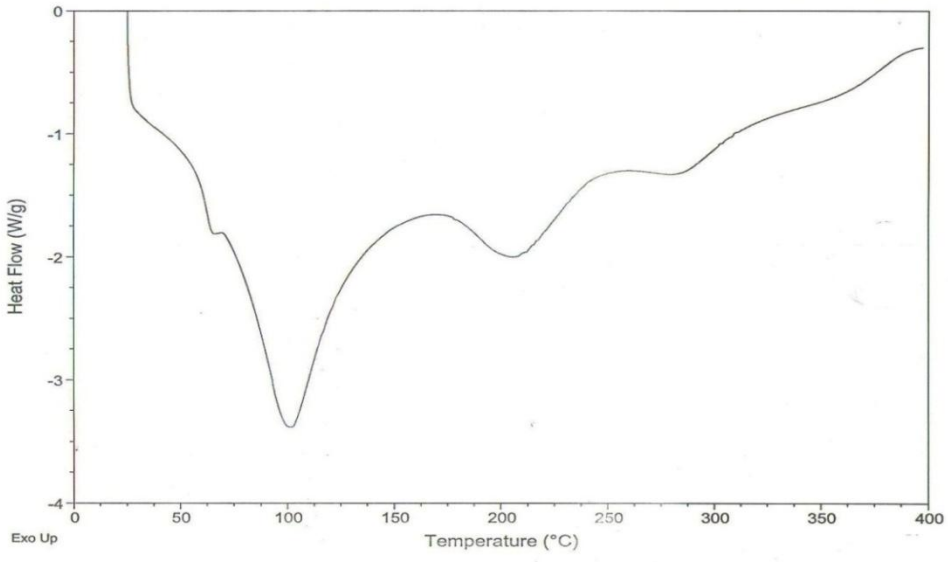

Figure 74: DSC thermogram of chitosan-polycarbophil IPEC

6.3.3.3 X-ray diffraction (XRD)

The X-ray diffraction pattern of chitosan is presented in figure 36. The X-ray diffraction pattern of chitosan powder showed two prominent diffraction peaks at 11° (2θ) and 20° (2θ). A shoulder peak appears at 22° (2θ) and also a minor peak appears at 27° (2θ). The two prominent crystalline peaks at 11° (2θ) and 20° (2θ) are typical fingerprints of chitosan which are related to the hydrated and anhydrous crystals respectively [215].The x-ray diffraction pattern of polycarbophil is shown in figure 75. The X-ray diffraction pattern of polycarbophil powder showed prominent diffraction peak at 19° (2θ) and minor peak appears at 29° (2θ).

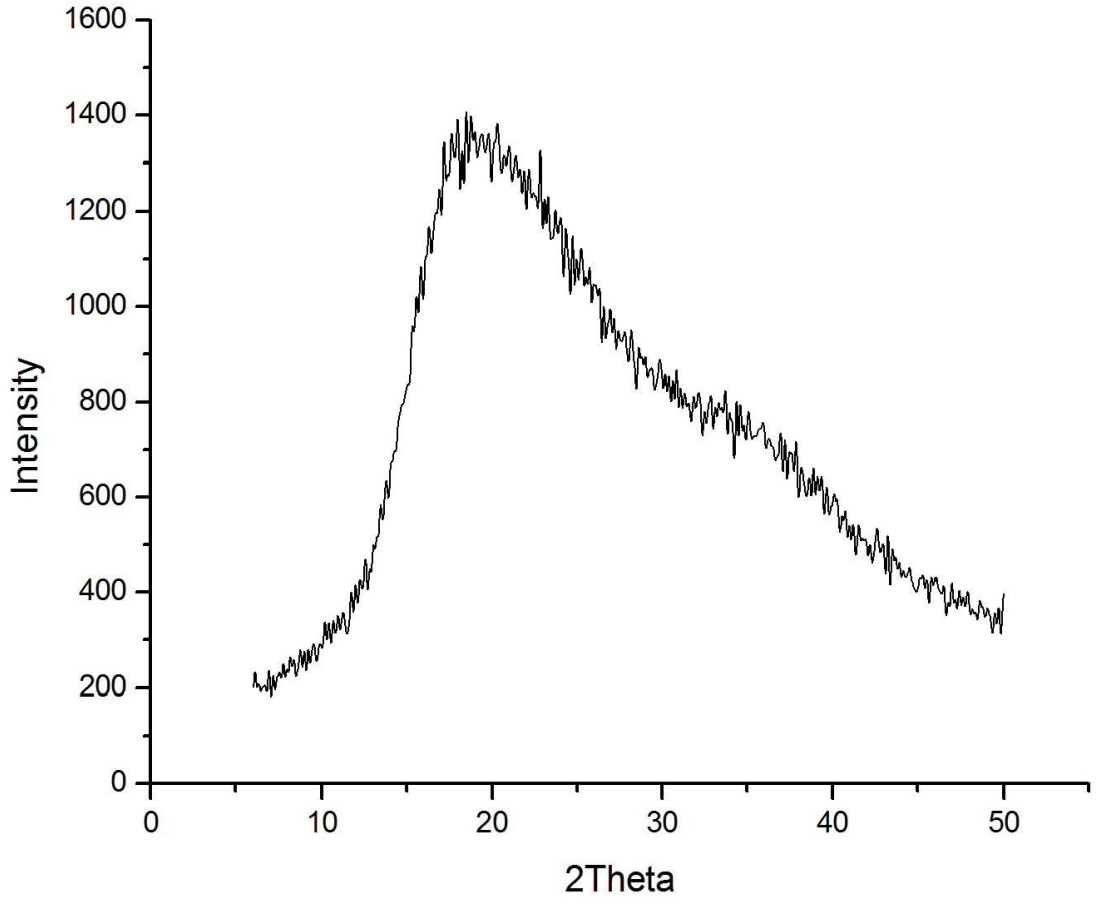

Figure 75: X-ray diffraction spectra of polycarbophil

IPEC X-ray diffraction pattern is given in figure 76. The X-ray diffraction pattern of IPEC powder exhibits prominent and broader diffraction peak at 20° (2θ) and minor peak at 31° (2θ). Thus, the XRD result reveals that introduction of the polycarbophil chains on the surface of the chitosan cause the breakdown of its crystallinity. The broad amorphous pattern of the IPEC indicates a good compatibility and strong interactions between polycarbophil and chitosan with a complete dispersion of chitosan chains. These intermolecular interactions could prevent macromolecules to crystallize individually as reported for some interpolymer complexes.

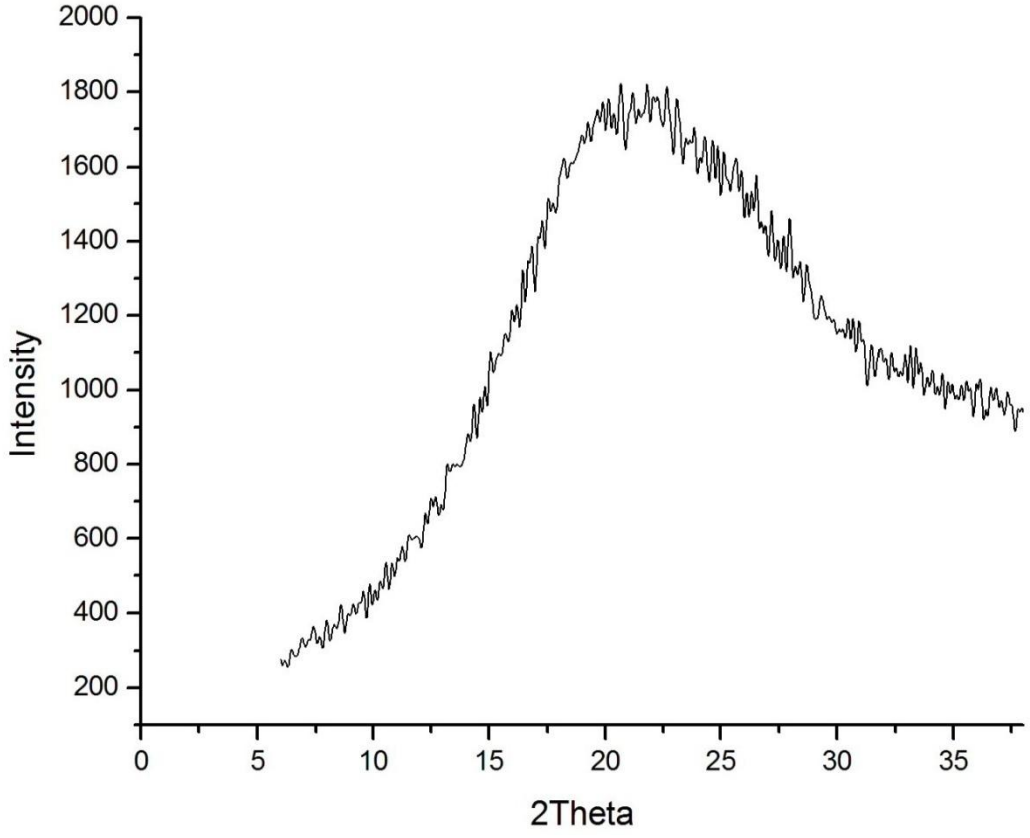

Figure 76: X-ray diffraction spectra of chitosan-polycarbophil IPEC

6.3.4 Evaluation of matrix tablets containing 5-fluorouracil (5-FU)

Tablet properties

The experimental results of tablet evaluation parameters are summarized in table 30. The weights of the prepared tablets were in the range of from 149.1 to 150.2 mg. Tablets of all the batches complied with the weight variation requirement of Indian pharmacopeia and no batch varied more than 10 % of the average weight indicating consistency in the preparation of tablet with minimal batch to batch variation [182]. Thickness of all the tablet formulations ranges from 2.01 to 2.02 mm. Hardness of the tablets ranged between 62-74 N. All tablet formulations exhibit friability less than 1%, indicating compliance with the requirement of USP 29 [183].

Table 30: Evaluation data of 5-FU matrix tablets

Formulation code	Weight (mg)* (n=20)	Thickness (mm)* (n=20)	Hardness (N)* (n=10)	Friability (%) (n=20)	%Drug content* (n=3)
FA1	149.1±0.44	2.01±0.02	62±3	0.15	99.93±0.05
FA2	149.2±0.64	2.02±0.01	65±2	0.13	99.90±0.05
FB1	150.2±0.57	2.01±0.02	60±4	0.11	99.93±0.01
FB2	149.2±0.43	2.01±0.02	64±3	0.12	99.91±0.05
FC1	149.5±0.42	2.02±0.01	74±2	0.04	99.89±0.05
FC2	149.4±0.43	2.01±0.02	70±3	0.08	99.90±0.09
FC3	149.2±1.00	2.01±0.02	72±3	0.09	99.91±0.08
FC4	150.0±0.57	2.02±0.02	73±2	0.05	99.92±0.04
FD1	150.1±1.00	2.02±0.02	73±3	0.06	99.92±0.05
FD2	149.2±0.42	2.02±0.01	74±2	0.06	99.94±0.01
FE1	150.1±0.53	2.02±0.02	74±2	0.03	99.95±0.05
FE2	149.2±0.43	2.01±0.01	74±1	0.04	99.92±0.05

***mean± Standard Deviation**

6.3.5 Swelling studies

The influence of pH of the buffer solution on the swelling behavior of formulations at 37±0.5 °C in phosphate buffer pH 6.8, simulated vaginal fluid pH 4.2 and phosphate buffer pH 6.8 are given in table 31,32,33 and graphically represented in figure 77A, 77B, 78A,78B and 79A, 79B respectively.

The swelling ratios of tablet formulations at different pH environment depend on the availability of the expanded polymer matrix, polymer chain relaxation, and availability of ionizable functional groups such as –COOH that can form hydrogen bonds with dissolution medium. Polycarbophil is an acrylic acid polymer loosely cross-linked with divinyl glycol. The swelling features in water depend both on pH and on the ionic strength of the solution. The swelling degree increases with increasing pH. The amount of water that the polymer may absorb ranges from 15-35 ml per gram, at acidic pH values, to 100 ml per gram, in neutral or basic medium [216]. Polycarbophil formulation exhibit least swelling in simulated vaginal fluid pH 4.2 than all other buffer solutions. As discussed earlier, there is gradual increase in swelling in vaginal pH 4.2, as carboxyl groups of polycarbophil tends to dissociate at a pH > 4.5, the osmotic pressure inside the hydrogels increases. Therefore, gradual rise in swelling occurred in the vaginal pH. However, in phosphate buffer pH 6.8, there is more dissociation of carboxylic acid than in pH 4.2, hence higher swelling is observed. Higher concentration of polycarbophil leads to higher swelling index in phosphate buffer pH 6.8. Near neutral pH polycarbophil containing polymers ionize to a greater extent and swells more. Hence, greater swelling index is seen in phosphate buffer pH 6.8 than in simulated vaginal fluid pH 4.2. In phosphate buffer pH 7.4 there is a sharp increase in the swelling of polycarbophil

polymer. As the acidic carboxyl group tends to readily interact with the basic medium, the rate of swelling is fast and there is increase in swelling index but less than the swelling index of phosphate buffer pH 6.8. This may be explained due to carboxylate group of polycarbophil ionizing rapidly in basic pH, whereas, in near neutral pH there is slow and gradual ionization that leads to highest swelling index. This is in agreement with the reported studies [217]. The physical mixture of chitosan and polycarbophil formulations exhibited high swelling index in simulated vaginal pH 4.2 owing to gel forming capacity of chitosan in acidic pH. In phosphate buffer pH 6.8 also, higher swelling index was observed due to the ionization of carboxylate ion of polycarbophil but deprotonation of amine group of chitosan occurs. This may lead to weaker electrostatic interaction and lesser attraction of polymer chains leading to more opened structure resulting in higher swelling index. Whereas in case of phosphate buffer pH 7.4, the polycarbophil formed gel around tablet rapidly as a result it hindered the chitosan swelling characteristic leading to highest swelling index. IPEC containing tablet formulations exhibited, a almost similar swelling index for all the buffer solutions. The similarity swelling profiles in both the buffer solutions may be attributed to the lack of availability of free functional group as in physical mixture of polymers or single polymers. However, IPEC containing formulations exhibited relatively lesser swelling index than polycarbophil alone. When less cross linked polycarbophil undergoes complexation with chitosan, the bulkiness increase and the lightly cross linked polycarbophil gets converted to highly coiled structure. This might be the reason why IPEC formulation exhibited lesser swelling index than polycarbophil alone. FD1 and FD2 formulations containing chitosan and polycarbophil along with IPEC exhibited swelling

index due to the availability of free functional groups of chitosan and polycarbophil polymers. The presence of polymers in low concentration didn't has ability for chain disentanglement or chain relaxation. Hence swelling appeared for all buffer solutions.

Table 31: Swelling index data of 5-FU formulations FA1-FE2 in phosphate buffer pH 6.8

Formulation Code	Swelling index Mean ± S.D*							
	Time in Hours							
	1 hour	2 hour	3 hour	4 hour	5 hour	6 hour	7 hour	8 hour
FA1	52 ±0.21	98 ±0.32	159 ±0.26	216 ±0.64	298 ±0.36	325 ±0.47	397 ±0.65	429 ±0.32
FA2	67 ±0.16	153 ±0.27	214 ±0.63	289 ±0.52	342 ±0.35	378 ±0.22	427 ±0.27	487 ±0.36
FB1	38 ±0.35	79 ±0.56	121 ±0.72	152 ±0.44	193 ±0.27	257 ±0.43	312 ±0.55	338 ±0.62
FB2	50 ±0.21	96 ±0.15	145 ±0.25	190 ±0.42	230 ±0.35	284 ±0.73	352 ±0.23	387 ±0.72
FC1	335 ±0.11	378 ±0.37	424 ±0.75	482 ±0.23	535 ±0.52	628 ±0.72	679 ±0.82	752 ±0.55
FC2	352 ±0.34	395 ±0.51	442 ±0.61	502 ±0.54	572 ±0.26	659 ±0.72	695 ±0.34	783 ±0.65
FC3	357 ±0.51	398 ±0.26	452 ±0.34	508 ±0.42	569 ±0.36	651 ±0.37	702 ±0.81	785 ±0.25
FC4	389 ±0.23	433 ±0.31	478 ±0.45	511 ±0.52	592 ±0.23	678 ±0.26	734 ±0.76	799 ±0.23
FD1	160 ±0.11	190 ±0.36	242 ±0.72	298 ±0.35	330 ±0.62	425 ±0.38	482 ±0.67	542 ±0.84
FD2	190 ±0.26	274 ±0.34	372 ±0.65	395 ±0.54	534 ±0.67	658 ±0.62	687 ±0.67	756 ±0.73
FE1	194 ±0.65	270 ±0.72	270 ±0.52	392 ±0.83	536 ±0.27	655 ±0.36	690 ±0.41	760 ±0.27
FE2	195 ±0.72	275 ±0.69	374 ±0.54	393 ±0.26	532 ±0.46	660 ±0.47	685 ±0.36	762 ±0.87

***Standard deviation, n = 3**

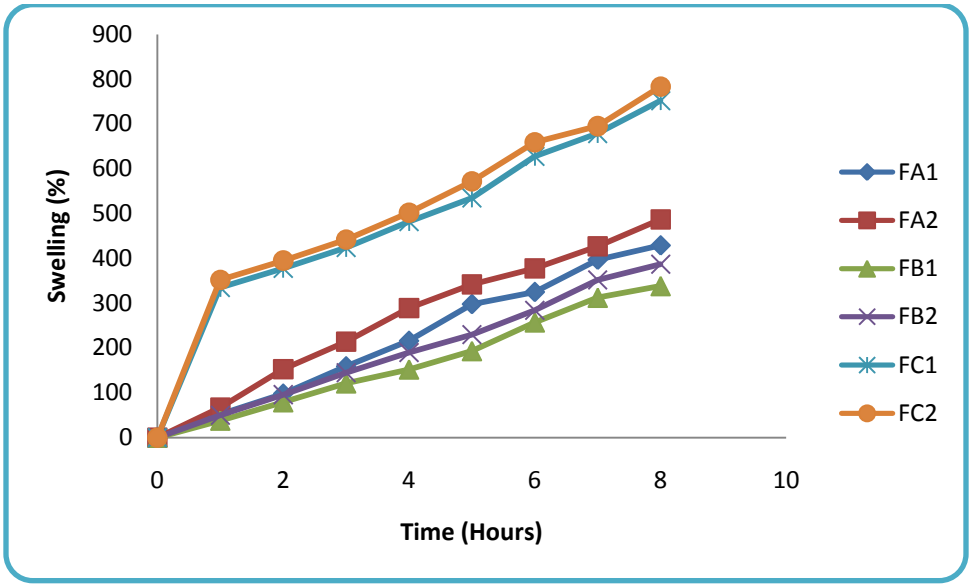

Figure 77A: Swelling index profile for 5-FU formulations FA1-FC2 in phosphate buffer pH 6.8

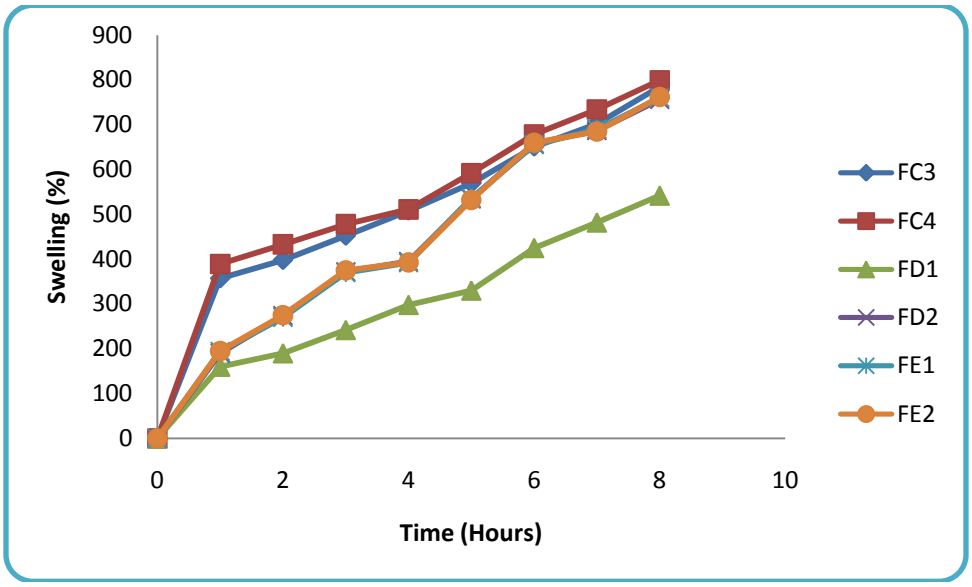

Figure 77B: Swelling index profile for 5-FU formulations FC3-FE2 in phosphate buffer pH 6.8

Table 32: Swelling index data of 5-FU formulations FA1-FE2 in SVF pH 4.2

Formulation Code	Swelling index Mean ± S.D*							
	Time in Hours							
	1 hour	2 hour	3 hour	4 hour	5 hour	6 hour	7 hour	8 hour
FA1	20 ±0.43	46 ±0.51	89 ±0.21	97 ±0.42	---	---	---	---
FA2	27 ±0.28	58 ±0.51	94 ±0.37	114 ±0.26	---	---	---	---
FB1	35 ±0.41	79 ±0.47	121 ±0.28	152 ±0.17	193 ±0.51	---	----	----
FB2	52 ±0.29	98 ±0.33	148 ±0.71	191 ±0.28	233 ±0.45	---	---	---
FC1	312 ±0.11	367 ±0.25	410 ±0.32	478 ±0.25	527 ±0.31	614 ±0.45	669 ±0.27	742 ±0.35
FC2	335 ±0.25	388 ±0.51	435 ±0.23	498 ±0.31	562 ±0.45	638 ±0.37	685 ±0.46	754 ±0.73
FC3	356 ±0.52	396 ±0.37	455 ±0.82	502 ±0.45	572 ±0.57	658 ±0.72	698 ±0.22	772 ±0.42
FC4	387 ±0.26	423 ±0.35	476 ±0.62	521 ±0.71	593 ±0.34	674 ±0.26	734 ±0.27	792 ±0.52
FD1	157 ±0.13	189 ±0.52	234 ±0.54	294 ±0.26	327 ±0.55	421 ±0.22	478 ±0.31	532 ±0.43
FD2	195 ±0.54	271 ±0.32	367 ±0.45	392 ±0.52	523 ±0.27	647 ±0.31	678 ±0.44	752 ±0.23
FE1	190 ±0.21	265 ±0.34	360 ±0.44	386 ±0.27	525 ±0.66	650 ±0.54	680 ±0.67	755 ±0.88
FE2	189 ±0.32	260 ±0.45	365 ±0.25	380 ±0.75	534 ±0.26	654 ±0.71	682 ±0.24	760 ±0.19

***Standard deviation, n = 3**

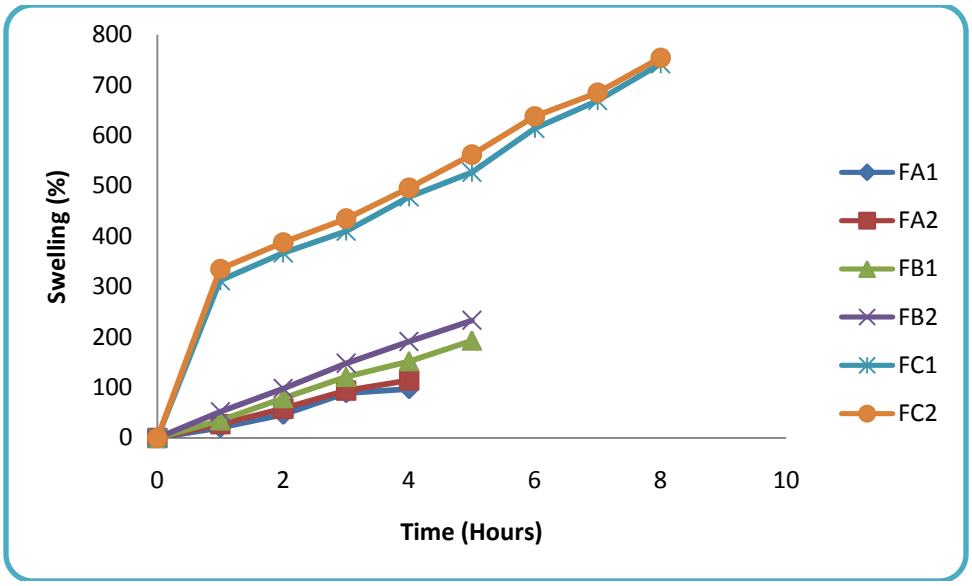

Figure 78A: Swelling index profile for 5-FU formulations FA1-FC2 in SVF pH 4.2

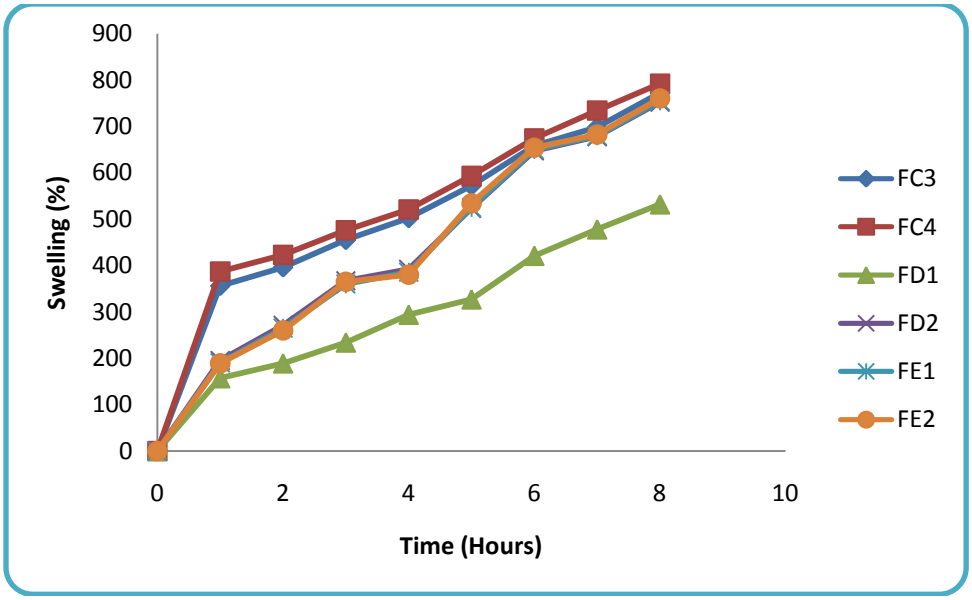

Figure 78B: Swelling index profile for 5-FU formulations FC3-FE2 in SVF pH 4.2

Table 33: Swelling index data of 5-FU formulations FA1-FE2 in phosphate buffer pH 7.4

Formulation Code	Swelling index Mean ± S.D*							
	Time in Hours							
	1 hour	2 hour	3 hour	4 hour	5 hour	6 hour	7 hour	8 hour
FA1	25 ±0.11	52 ±0.34	94 ±0.23	102 ±0.52	148 ±0.26	179 ±0.62	---	----
FA2	41 ±0.61	67 ±0.45	108 ±0.28	124 ±0.82	164 ±0.72	186 ±0.38	---	----
FB1	18 ±0.38	39 ±0.52	70 ±0.38	98 ±0.74	121 ±0.47	---	----	---
FB2	50 ±0.47	96 ±0.37	128 ±0.46	181 ±0.57	193 ±0.67	----	---	----
FC1	310 ±0.84	361 ±0.37	404 ±0.67	462 ±0.34	518 ±0.72	611 ±0.45	659 ±0.37	739 ±0.48
FC2	330 ±0.32	385 ±0.62	429 ±0.16	493 ±0.17	560 ±0.38	625 ±0.71	683 ±0.28	757 ±0.11
FC3	352 ±0.25	398 ±0.43	458 ±0.84	512 ±0.38	582 ±0.73	668 ±0.87	702 ±0.38	782 ±0.82
FC4	384 ±0.77	443 ±0.38	482 ±0.47	525 ±0.31	597 ±0.62	678 ±0.71	724 ±0.68	797 ±0.28
FD1	183 ±0.11	228 ±0.38	286 ±0.37	378 ±0.54	411 ±0.71	447 ±0.27	489 ±0.33	512 ±0.41
FD2	295 ±0.34	329 ±0.25	394 ±0.62	478 ±0.38	543 ±0.86	625 ±0.27	691 ±0.48	745 ±0.38
FE1	289 ±0.26	318 ±0.35	389 ±0.18	445 ±0.71	534 ±0.46	621 ±0.73	687 ±0.28	740 ±0.77
FE2	290 ±0.24	320 ±0.83	390 ±0.28	471 ±0.87	541 ±0.68	622 ±0.92	692 ±0.67	743 ±0.55

***Standard deviation, n = 3**

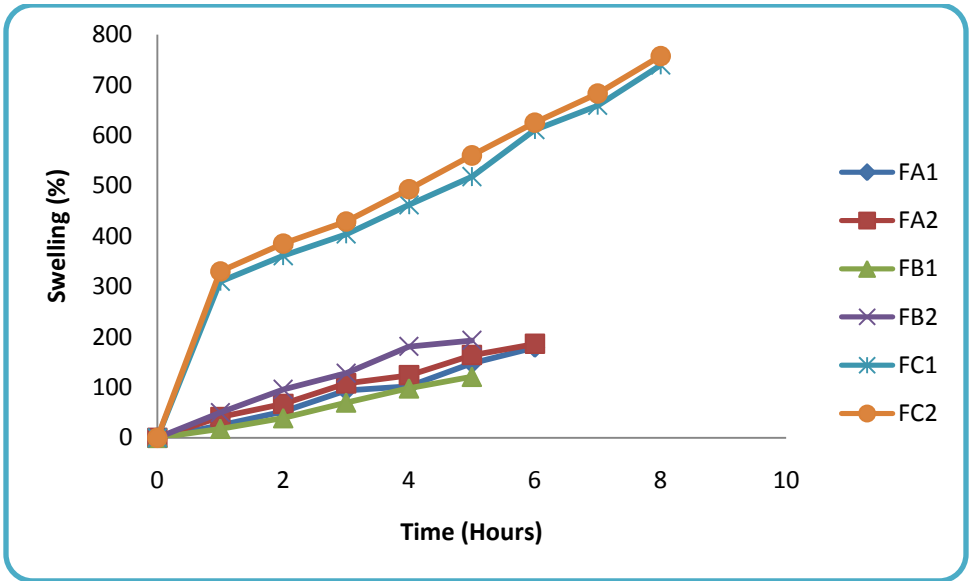

Figure 79A: Swelling index profile for 5-FU formulations FA1-FC2 in phosphate buffer pH 7.4

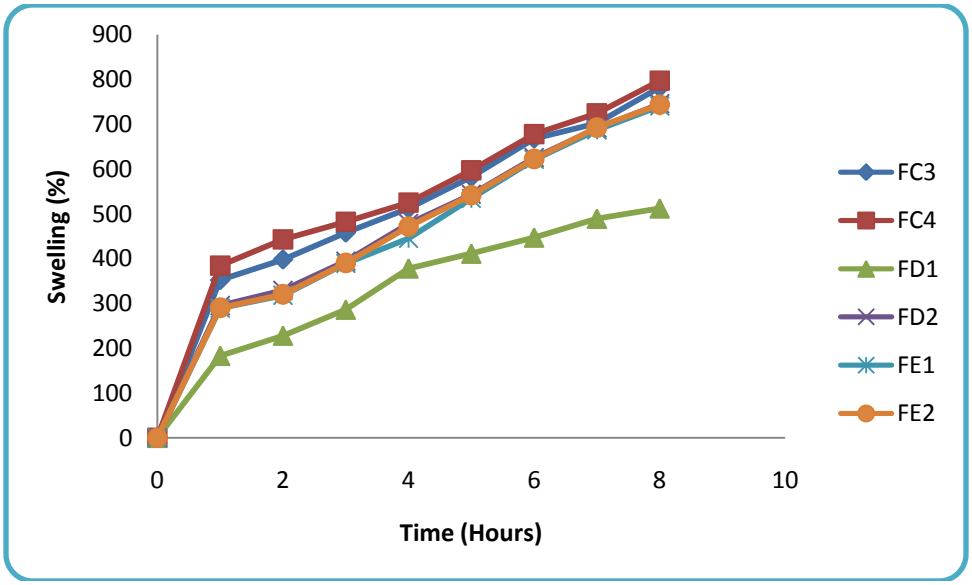

Figure 79B: Swelling index profile for 5-FU formulations FC3-FE2 in phosphate buffer pH 7.4

6.3.6 *In vitro* dissolution studies

The dissolution data of the individual formulations in phosphate buffer pH 6.8, simulated vaginal fluid pH 4.2 and phosphate buffer pH 7.4 are shown in the table 34, 35 and 36 respectively and graphical represented are given in figures 80A, 80B, 81A,81B and 82A, 82B respectively.

During dissolution, the external surface of tablets containing hydrated polycarbophil, swelled and formed gel layer (hydrogel) that might have controlled the release of the drug from the tablets. In acidic pH, polycarbophil forms less gel layer due to minimal dissociation of carboxylate groups. Hence the drug release do not sustain for longer period of time. Polycarbophil formed discrete microgel made up of number of polymer particles into which 5-fluorouracil (5-FU) was dispersed. In phosphate buffer pH 6.8, polycarbophil exhibited highest dissolution and hydrogel was fully hydrated. Polycarbophil polymer forms "fishnet" gel structure upon hydration due to few crosslink sites to constrain the polymer. Consequently, the interstitial spaces between the swollen gel particles were eliminated, and there was no significant difference between the micro and macroviscosity. This homogeneous gel structure provided significant resistance to diffusion of 5-fluorouracil. Thus 5-fluorouracil was released in linear manner. Drug release rates were affected by differences in the rates of hydration and swelling of the polymer hydrogel, which are dependent on the molecular structure of the polymers, including crosslink density, chain entanglement, and crystallinity of the polymer matrix [218].Whereas in case of phosphate buffer pH 7.4, the polycarbophil polymer swelled up rapidly due to exposure to basic medium (pH 7.4) where carboxylate ion of polycarbophil are readily ionized and also higher solubility of 5-fluorouracil in phosphate buffer pH 7.4

ease for rapid escape. Hence rate of 5-fluorouracil is little rapid than phosphate buffer pH 7.4 [219]. The physical mixture of chitosan and polycarbophil did not produce the desired drug release. This may be due to faster disentanglement of the polymeric chains during water uptake into the matrix systems when the polymers are not cross-linked with each other, resulting in fast drug release. There is faster 5-fluorouracil release from tablets based on chitosan-polycarbophil powder mixture in simulated vaginal fluid pH 4.2 compared to phosphate buffer pH 6.8 and pH 7.4. Inspite of gel forming capacity of chitosan at acidic pH, the presence of polycarbophil doesn't produce synergistic effect. The physical mixture of chitosan and polycarbophil release about 90% of drug in 5 h only [220]. Whereas in phosphate buffer pH 6.8 and 7.4 there is gradual drug release due to ability of polycarbophil carboxylate ion to dissociate and form gel. This indicates that although the tablets are based on dry blend of polymers, they are not able to achieve the desired drug release. 5-fluorouracil release rate from IPEC matrix was lower than that from physical mixture or polymer alone. IPEC containing formulation on contact with phosphate buffer pH 6.8 or 7.4 or simulated vaginal fluid pH 4.2 undergo swelling-driven phase transition from a glassy state to rubbery state. Inspite of higher swelling index of IPEC polymers, the matrix tablets were able to sustain the drug release. This may be due to more complex fishnet gel layer around that drug which released slowly over period of 8 h [221]. The presence of both cation and anion in the IPEC acts independently irrespective of buffer pH. Increase in the concentration of IPEC in tablets further retard the drug release to a little extent due to the formation of strong polymeric network. The presence of chitosan in IPEC tablets (FD1 formulation) exhibited rapid initial drug release only in phosphate buffer pH 6.8. This may be due to less concentration of

chitosan tend to escape from the gel layer and also the high drug solubility favor for high drug release profile. Whereas, the dissolution profile of FD2 formulation in phosphate buffer pH 6.8, inhibit the rapid initial release this may be due to the high polycarbophil concentration.FE1 and FE2 formulation containing similar polymer concentration as FD2 formulation but with an addition of sodium deoxycholate, acts as permeation enhancer. The drug release profile from FE1 and FE2 formulation exhibits similar drug release profile as FD2 formulation. Hence the presence of permeation enhancer doesn't have influence on drug release profile which is in agreement with the reported studies [222].

The above results showed the advantage of IPEC for monolithic formulations. The IPEC excipients, can afford controlled release of 5-fluorouracil in all study buffer solution. Only the presence of chitosan in lower concentration in IPEC matrix tablets has impact on drug release profile. However, addition of chitosan and polycarbophil in higher concentration to IPEC matrix tablets doesn't alter the drug release profile to a major extent. To confirm the similarity of FE2 formulation dissolution profiles in phosphate buffer pH 6.8, simulated vaginal fluid pH4.2 and phosphate buffer pH 7.4, the similarity factor (f_2) was calculated and summarized in the table 37.

Table 34: *In vitro* dissolution data of 5-FU formulations FA1-FE2 in phosphate buffer pH 6.8

Formulation Code	Drug Release (%)							
	1 hour	2 hour	3 hour	4 hour	5 hour	6 hour	7 hour	8 hour
	Mean ± S.D*							
FA1	13.17 ±0.84	29.28 ±1.13	41.37 ±0.92	59.38 ±0.73	70.36 ±0.28	82.77 ±0.58	90.22 ±0.25	95.35 ±0.73
FA2	11.23 ±0.52	19.52 ±0.26	29.11 ±0.74	37.25 ±0.85	42.65 ±0.82	54.27 ±0.75	67.27 ±1.18	78.26 ±0.83
FB1	44.23 ±0.73	58.18 ±0.87	76.32 ±1.27	88.23 ±0.37	95.27 ±1.19	98.27 ±0.46	----	----
FB2	32.73 ±0.92	43.87 ±0.75	65.29 ±0.28	74.72 ±0.38	82.46 ±0.97	89.47 ±1.36	94.27 ±0.37	----
FC1	23.46 ±0.48	40.82 ±1.37	53.94 ±0.48	62.56 ±0.37	76.36 ±1.47	86.38 ±0.97	95.37 ±0.52	98.47 ±0.22
FC2	20.53 ±0.67	35.27 ±0.87	48.22 ±1.36	58.83 ±0.95	70.47 ±0.53	82.11 ±0.92	91.34 ±0.62	94.63 ±0.82
FC3	11.23 ±0.87	24.57 ±0.32	34.74 ±0.28	45.38 ±0.17	56.82 ±0.58	72.58 ±0.28	86.98 ±0.71	93.22 ±0.11
FC4	8.58 ±0.93	14.22 ±1.34	24.87 ±0.78	37.18 ±0.91	48.28 ±0.54	62.47 ±0.82	70.49 ±0.57	77.28 ±0.47
FD1	40.38 ±0.11	46.35 ±0.21	55.21 ±0.47	67.22 ±0.83	85.31 ±0.92	95.47 ±0.47	96.98 ±0.21	98.36 ±0.52
FD2	13.75 ±0.58	20.51 ±0.94	35.92 ±0.63	52.57 ±0.93	67.11 ±1.05	76.32 ±0.86	90.15 ±0.18	97.27 ±0.85
FE1	12.36 ±0.96	21.57 ±0.17	34.78 ±0.48	53.11 ±0.92	68.86 ±1.13	77.21 ±0.25	90.82 ±0.17	97.26 ±0.24
FE2	12.48 ±0.24	22.32 ±0.94	35.67 ±0.28	54.38 ±0.73	69.57 ±0.89	76.38 ±1.04	91.25 ±0.57	97.58 ±0.62

***Standard deviation, n = 3**

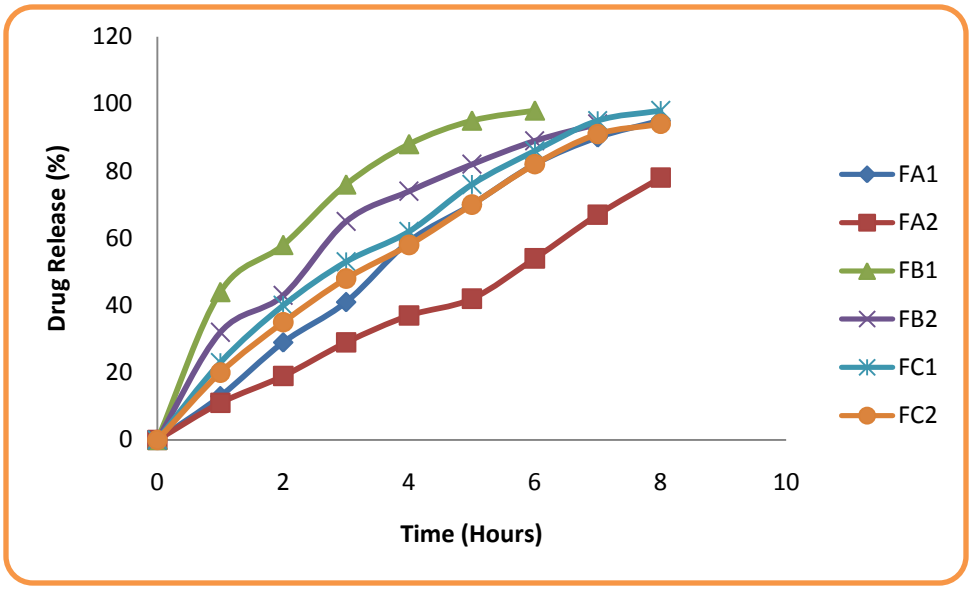

Figure 80A: 5-FU release profile of FA1-FC2 formulations in phosphate buffer pH 6.8

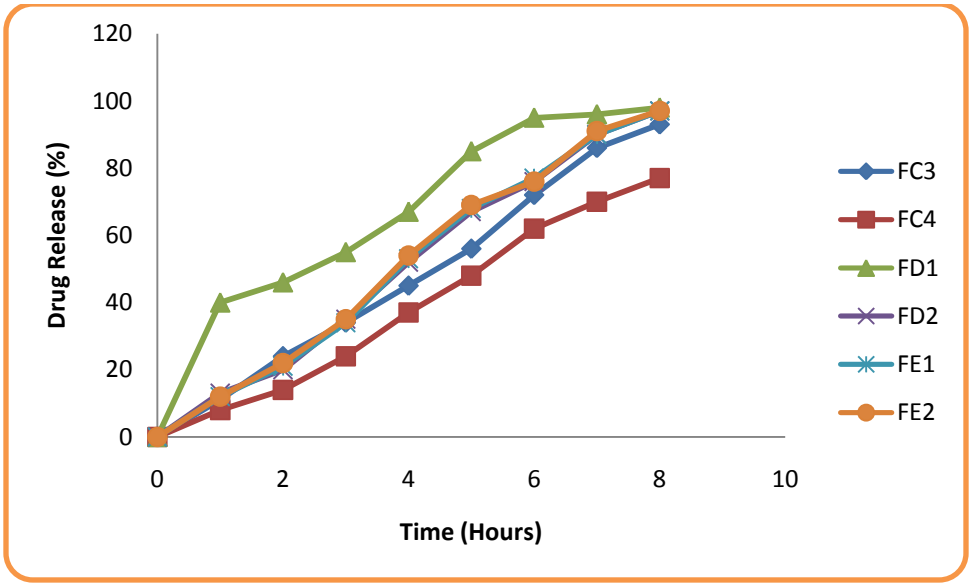

Figure 80B: 5-FU release profile of FC3-FE2 formulations in phosphate buffer pH 6.8

Table 35: *In vitro* dissolution data of 5-FU formulations FA1-FE2 in SVF pH 4.2

Formulation Code	Drug Release (%)							
	1 hour	2 hour	3 hour	4 hour	5 hour	6 hour	7 hour	8 hour
	Mean ± S.D*							
FA1	49.34 ±0.56	67.32 ±0.26	86.16 ±0.19	95.31 ±0.84	----	----	----	----
FA2	40.28 ±0.73	60.28 ±1.34	76.54 ±0.58	87.58 ±0.92	96.42 ±0.68	----	----	----
FB1	35.12 ±0.38	56.24 ±0.91	73.11 ±0.78	84.27 ±0.82	95.37 ±0.27	----	----	-----
FB2	20.37 ±0.93	48.28 ±0.49	69.55 ±1.28	80.38 ±0.39	94.22 ±0.62	----	----	----
FC1	24.25 ±0.28	39.58 ±0.36	53.62 ±0.92	65.85 ±0.21	74.58 ±0.58	83.26 ±0.95	93.28 ±1.04	98.27 ±0.53
FC2	20.41 ±0.57	34.11 ±0.28	51.54 ±0.48	60.38 ±0.21	72.35 ±0.48	80.38 ±1.21	91.32 ±0.93	94.22 ±0.32
FC3	10.47 ±0.32	27.52 ±0.81	35.18 ±0.23	47.28 ±0.28	59.32 ±0.65	74.21 ±0.72	88.37 ±1.21	93.25 ±0.37
FC4	8.21 ±0.37	13.21 ±0.52	22.15 ±0.71	35.18 ±0.82	47.37 ±0.91	64.21 ±0.26	70.17 ±0.72	76.21 ±0.85
FD1	20.17 ±0.37	31.46 ±0.28	43.27 ±0.79	57.32 ±0.93	64.22 ±0.21	75.28 ±0.16	81.24 ±0.72	86.27 ±0.11
FD2	11.21 ±0.71	19.83 ±0.32	34.27 ±0.91	50.82 ±1.21	62.17 ±0.38	69.21 ±0.57	87.22 ±0.71	97.27 ±0.92
FE1	10.18 ±0.85	19.46 ±0.92	34.72 ±0.77	50.26 ±0.14	62.18 ±0.26	69.27 ±1.36	88.28 ±0.62	98.27 ±0.72
FE2	11.21 ±0.85	20.17 ±0.38	35.28 ±0.92	51.37 ±0.65	63.26 ±0.52	74.28 ±0.72	88.32 ±0.26	98.26 ±0.82

***Standard deviation, n = 3**

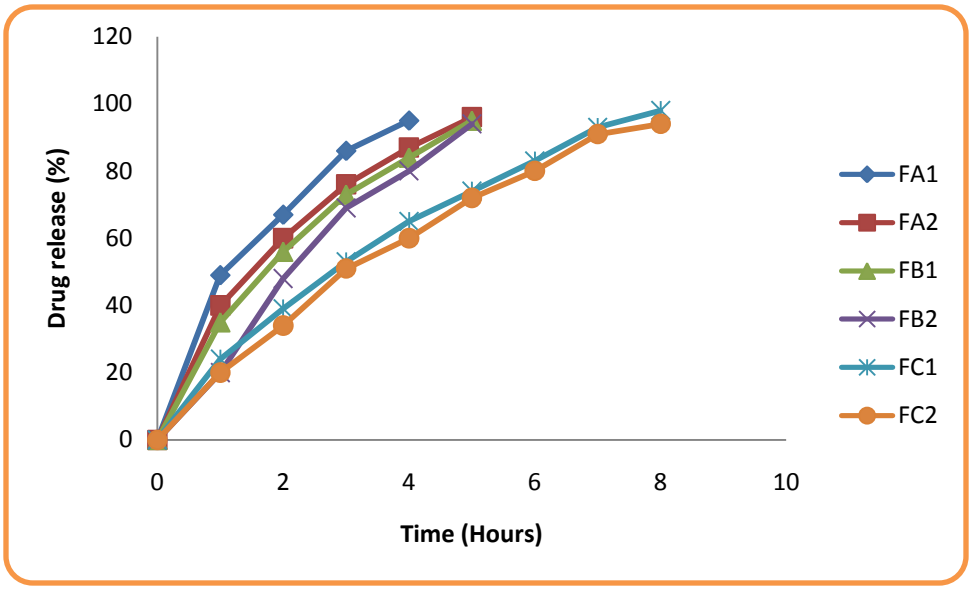

Figure 81A: 5-FU release profile of FA1-FC2 formulations in SVF pH 4.2

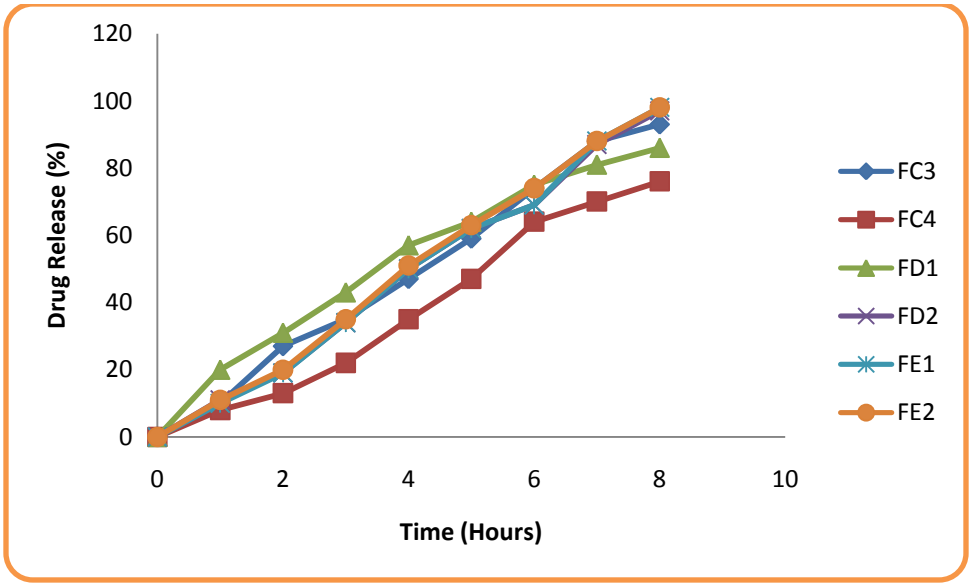

Figure 81B: 5-FU release profile of FC3-FE2 formulations in SVF pH 4.2

Table 36: *In vitro* dissolution data of 5-FU formulations FA1-FE2 in phosphate buffer pH 7.4

Formulation Code	Drug Release (%)							
	1 hour	2 hour	3 hour	4 hour	5 hour	6 hour	7 hour	8 hour
	Mean ± S.D*							
FA1	21.57 ±0.58	48.28 ±0.97	69.92 ±1.19	82.18 ±0.87	90.72 ±0.29	95.77 ±0.82	----	----
FA2	16.76 ±0.34	38.28 ±0.57	60.92 ±0.99	76.28 ±0.23	87.26 ±0.33	94.28 ±0.27	----	-----
FB1	32.17 ±0.72	57.28 ±0.89	75.28 ±0.28	87.72 ±0.32	95.76 ±0.51	----	----	----
FB2	21.64 ±0.62	49.72 ±0.27	72.37 ±0.92	83.26 ±0.97	96.25 ±0.37	----	----	----
FC1	24.47 ±0.58	38.28 ±0.22	53.77 ±0.37	62.36 ±0.97	75.82 ±0.22	84.22 ±0.18	94.18 ±0.19	98.22 ±0.72
FC2	19.46 ±0.38	33.28 ±0.19	45.28 ±0.18	57.92 ±0.92	70.38 ±0.17	80.27 ±0.23	91.62 ±0.12	94.28 ±0.39
FC3	16.66 ±0.37	26.47 ±0.91	37.28 ±0.19	45.27 ±0.18	58.21 ±0.95	75.21 ±0.78	84.12 ±0.18	96.18 ±0.82
FC4	9.38 ±0.92	15.24 ±0.37	23.57 ±0.22	35.28 ±0.52	48.22 ±0.92	61.23 ±0.38	73.26 ±0.49	75.34 ±0.73
FD1	10.57 ±0.47	16.38 ±0.38	25.85 ±0.82	38.28 ±1.35	56.28 ±0.83	68.27 ±0.28	80.92 ±0.10	89.27 ±0.32
FD2	13.23 ±0.49	20.47 ±0.93	35.11 ±0.12	52.91 ±1.21	65.48 ±0.29	72.12 ±0.82	90.84 ±0.24	97.42 ±0.23
FE1	13.11 ±0.23	21.27 ±0.95	35.57 ±0.57	52.34 ±0.28	64.92 ±0.87	73.87 ±0.32	91.42 ±0.63	96.22 ±0.83
FE2	14.22 ±0.34	20.47 ±1.63	34.21 ±0.47	51.57 ±0.38	63.28 ±0.81	72.41 ±0.18	90.27 ±0.52	96.32 ±0.24

***Standard deviation, n = 3**

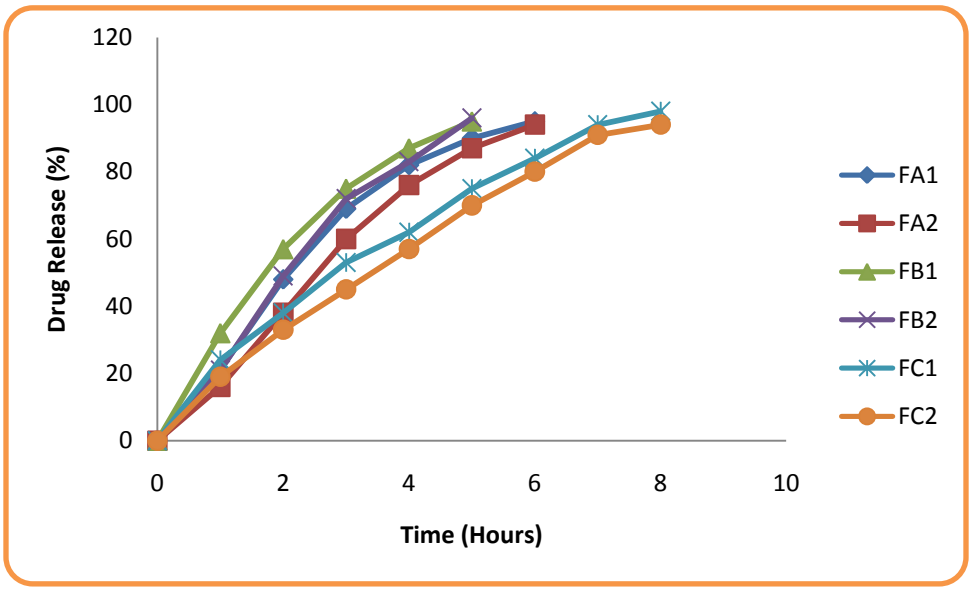

Figure 82A: 5-FU release profile of FA1-FC2 formulations in phosphate buffer pH 7.4

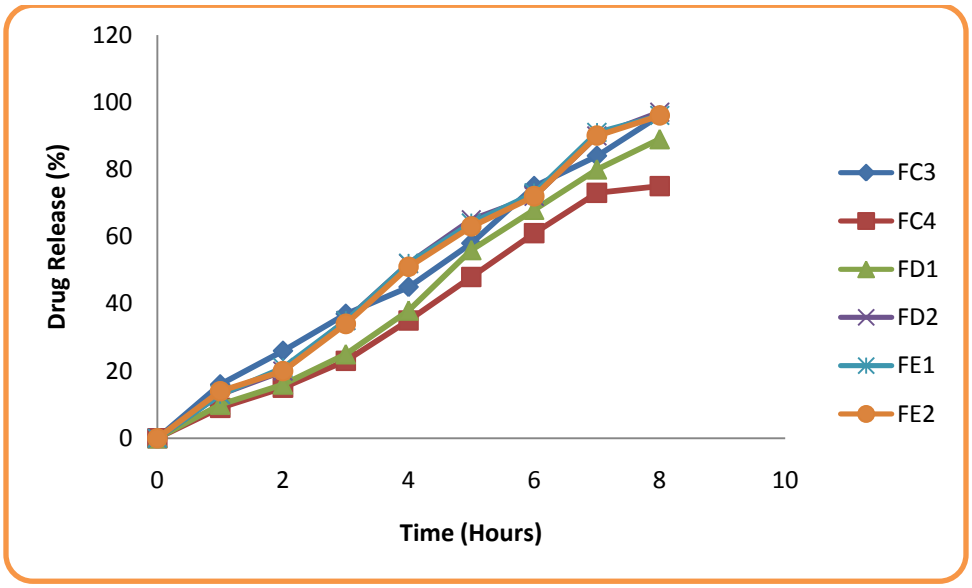

Figure 82B: 5-FU release profile of FC3-FE2 formulations in phosphate buffer pH 7.4

Table 37: Similarity factor (f_2) values calculated for the dissolution profiles of FD2 formulation between different buffer solutions.

Comparison	Similarity factor (f_2)
FD2(Buccal pH) vs FD2 (Vaginal pH)	76.21
FD2 (Buccal pH) vs FD2 (Rectal pH)	75.15

Since the f_2 values were higher than 50 (as per USFDA guidelines), these results confirmed that the drug release profiles were almost similar for FD2 formulation for buccal, vaginal and rectal pH.

6.3.7 *In vitro* mucoadhesion studies

Mucoadhesive strength of formulations FC1-FE2 are summarized in table 38 and represented in figure 83 respectively. Based on the *in vitro* desired drug release profile, formulations FC1-FE2 were subjected for the mucoadhesive studies. Four formulations containing IPEC exhibited the least mucoadhesive strength. The formed complex lacked the functional groups which are involved in the complex formation; hence they exhibited less mucoadhesive strength. Further increase in the concentration of IPEC, did not increase bioadhesive strength. The formed complex lacked strong binding but found little binding to the mucosal surface via hydrogen bonding interactions [189]. FD1 formulation containing chitosan and polycarbophil exhibited the higher mucoadhesive strength than IPEC formulation. The bioadhesion may be due to various reasons, the presence of a great number of carboxylic groups which provide the ability to form hydrogen bonds is a critical characteristic that is found in polycarbophil polymer and also may be due to the chain penetration of polymers in mucin. Increasing concentration of chitosan and

polycarbophil further increases bioadhesion. The presence of permeation enhancer in FE1 and FE2 formulation doesn't produce further mucoadhesion.

Table 38: Mucoadhesive strength data for FC1-FE2 formulations

Formulation code	Mucoadhesive strength(N/cm^2) Mean±SD*
FC1	0.03±0.01
FC2	0.05±0.021
FC3	0.05±0.02
FC4	0.06±0.032
FD1	0.12±0.027
FD2	0.25±0.03
FE1	0.24±0.03
FE2	0.25±0.02

***mean±SD, n=3**

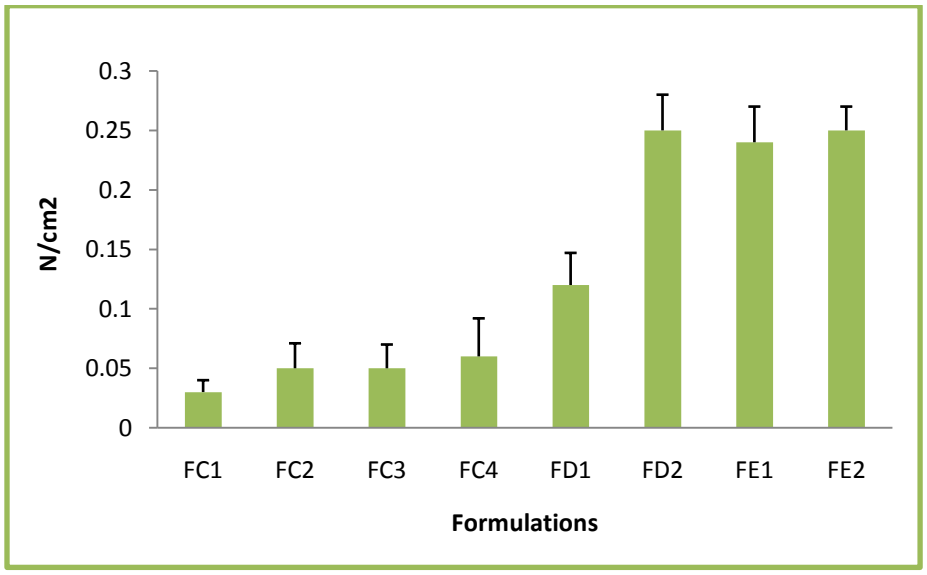

Figure 83: Mucoadhesive strength profile for FC1-FE2 formulations

6.3.8 *In vivo* X-ray studies

The bioadhesion & retention property was studied in albino rabbit. Optimized formulation FE2, developed by using barium sulfate (replacing 20 mg of 5-fluorouracil) was administered to the rabbit. The duration of tablet in buccal, vaginal and rectal cavity was monitored by radiograms. It is evident from the pictures (figure 84) that the tablets remained intact and adhered to the buccal, vaginal and rectal mucous membrane for over 8 Hrs.

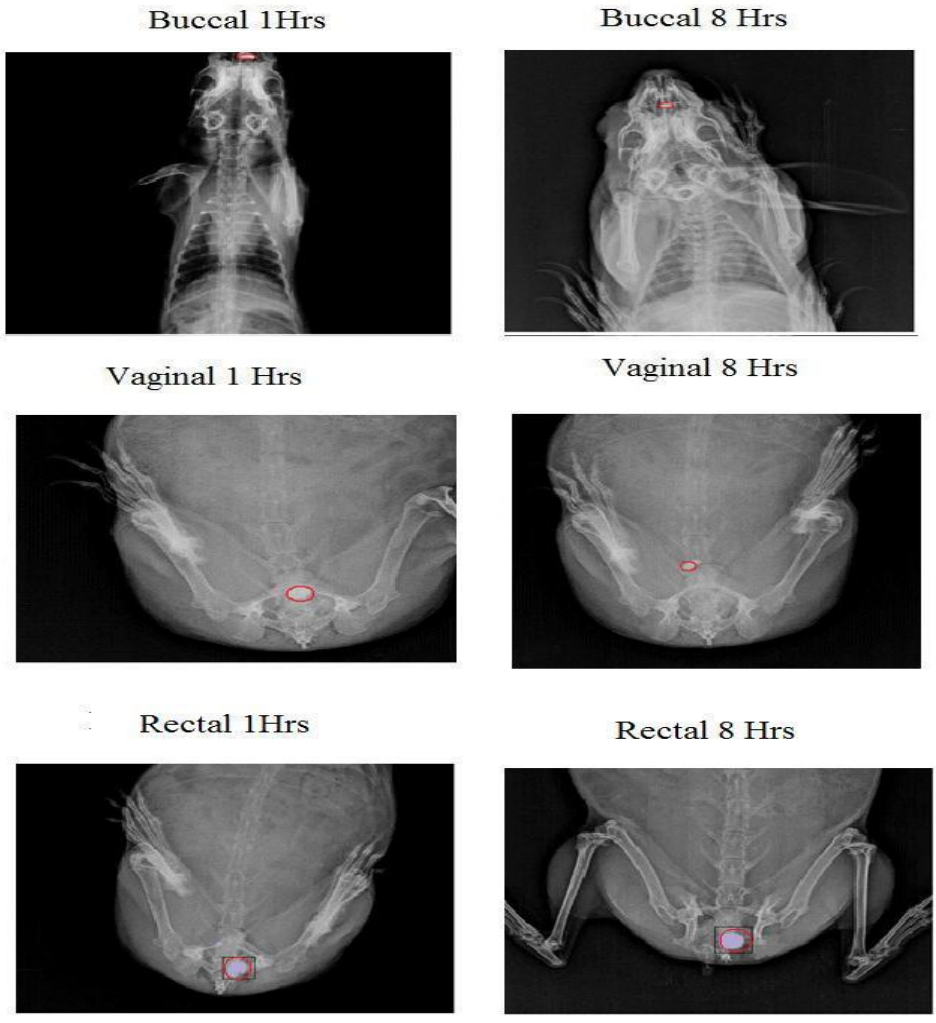

Figure 84: X-ray radiographic images of buccal, vaginal and rectal cavity at 1 and 8 h after ingestion of $BaSO_4$-loaded optimized FE2 matrix tablet in rabbits

6.3.9 Ex vivo permeation studies

5-FU permeation from formulations FE1 and FE2 across sheep mucosa over a period of 8 h is shown in Figure 85 and summarized in table 39. The maximum permeation of 5-FU from FE2 was 97 % at 8 h compared with 63 % from FE1. Regression of the linear portions of the two plots gave Slopes and intercepts from which the permeation flux (slope divided by mucosal surface area) of F5 and F6 were calculated to be 8.5866 and 5.1333 $mg/cm^2/h$, respectively. In formulation FE1 addition of 2 % SDC increased the cumulative percentage of drug permeation to 63 %. This may be due to extraction of only mucosal lipid from the intercellular spaces by SDC. Thus, this enhances the diffusivity of the 5-FU via the par cellular or polar route. Further increase in concentration of SDC (FE2), i.e., 3 %, increased the drug permeation up to 97 % thus SDC in 3 % extract lipids from the cell membranes, along with the extraction of mucosal lipid from the intercellular spaces by the formation of micelles. This resulted in enhancing passive diffusivity of the 5-FU via transcellular (crossing the cell membranes and entering the cell) and par cellular routes [223]. It was mentioned that SDC can also cause the uncoiling and extension of the protein helices, which leads to opening of the polar pathways for diffusion [224]. All these effects might contribute to enhancing the permeation of the drug.

Table 39: 5-FU permeation data for FE1 and FE2 formulations.

Formulation Code	Drug permeated (%)							
	1 hour	2 hour	3 hour	4 hour	5 hour	6 hour	7 hour	8 hour
	Mean ± S.D*							
FE1	8.23 ±0.58	14.69 ±1.37	21.42 ±1.25	27.62 ±0.93	35.39 ±0.38	43.57 ±0.92	54.24 ±1.12	63.25 ±0.92
FE2	17.32 ±1.42	29.73 ±0.94	42.82 ±0.92	57.38 ±0.83	73.21 ±1.25	89.51 ±0.82	95.21 ±0.95	97.21 ±1.11

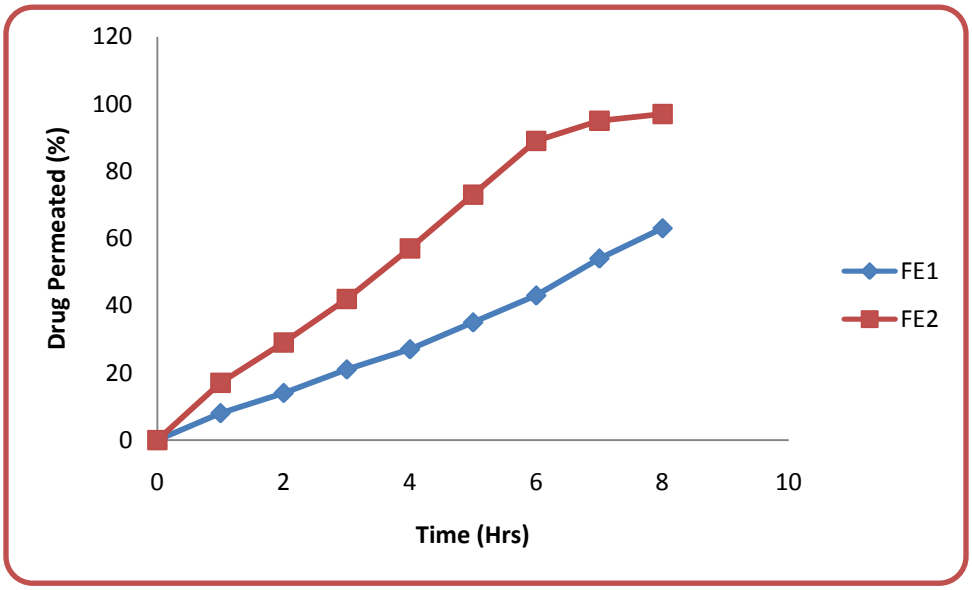

Figure 85: 5-FU permeation profiles of FE1 and FE2 formulations

6.3.10 Mathematical model fitting

To ascertain drug release mechanism and release rate, the release data were fitted into release models using PCP Disso V2.01 dissolution software. The parameters like 'n' the time exponent and 'R' the regression co-efficient were determined to know the release mechanisms. The data for the formulations FC1-FD2 are summarized in table 40.

Table 40: Mathematical model fitting data for FC1 to FD2 formulations

Formulation code	Buffer condition	Zero order R	First order R	Matrix R	Peppas		Hixon crowel R
					R	n	
FC1	Buccal pH	0.9820	0.9862	0.9740	0.9991	0.7679	0.9849
	Vaginal pH	0.9708	----	0.9830	0.9993	0.7172	0.8872
	Rectal pH	0.9729	----	0.9812	0.9991	0.7160	0.8875
FC2	Buccal pH	0.9896	0.9924	0.9651	0.9994	0.8197	0.9915
	Vaginal pH	0.9795	0.9387	0.9739	0.9974	0.7951	0.9858
	Rectal pH	0.9879	0.9199	0.9663	0.9992	0.8130	0.9768
FC3	Buccal pH	0.9967	0.9952	0.9128	0.9989	0.8820	0.9958
	Vaginal pH	0.9974	0.9049	0.9240	0.9940	0.7876	0.9557
	Rectal pH	0.9977	0.8089	0.9322	0.946	0.8955	0.9209
FC4	Buccal pH	0.9912	0.9897	0.8931	0.9956	0.8116	0.9902
	Vaginal pH	0.9784	0.9015	0.8642	0.9912	0.8876	0.9344
	Rectal pH	0.9904	0.9506	0.8978	0.9923	0.8230	0.9684
FD1	Buccal pH	0.9376	0.9466	0.9857	0.9752	0.8560	0.9437
	Vaginal pH	0.9800	0.9828	0.9742	0.9980	0.7639	0.9975
	Rectal pH	0.9896	0.9031	0.8903	0.9902	0.8560	0.9460
FD2	Buccal pH	0.9967	0.9947	0.9141	0.9928	0.8836	0.9951
	Vaginal pH	0.9971	0.8068	0.9119	0.9962	0.9334	0.9159
	Rectal pH	0.9966	---	0.9211	0.9929	0.9048	0.8663

The FD2 formulation is considered as the best formulation based on the *in vitro* drug release studies and the bioadhesion studies. The best model fit for FD2 formulation is zero order and the n value in peppas model is between 0.9-1 indicating non-fickian diffusion as the release mechanism.

6.3.11 Stability studies

Stability studies of 5-FU tablet formulation FE2 was carried out to determine the physical stability of the formulation. The stability studies were carried out at 25±2 °C and 60±5 % RH, 30±2 °C and 65±5 % RH and 40±2 °C and 75±5 % RH for 6 months. The 5-FU content in the formulation was evaluated. The observation of conditions is shown in table 41. There was no significant change in the tablet properties and drug content.

Table 41: Stability studies data for FE2 formulation

Sampling interval (Months)	Stability study conditions		
	25±2 °C & 60±5 % RH	30±2 ºC & 65±5 % RH	40±2 ºC & 75±5 % RH
	% Drug content mean ± S.D*		
0	99.8± 0.62	99.8 ± 0.33	99.8 ± 0.81
3	98.8± 0.15	98.4 ± 0.43	98.2± 0.52
6	98.1± 0.16	97.9 ± 0.72	98.2 ± 0.32

***Standard deviation, n = 3**